Characterization and Application of Nanomaterials (2022) Volume 5 Issue 1
doi: 10.24294/can.v5i1.1412

ORIGINAL RESEARCH ARTICLE

Preparation of MOF/Au composite nanoparticles and their SERS properties

Huihui Liu, Baichuan Zhao, Congyun Zhang*

School of Materials Science and Engineering, North University of China, Taiyuan 030051, Shanxi Province, China.
E-mail: z.congyun@nuc.edu.cn

ABSTRACT

Surface-enhanced Raman scattering (SERS) spectrum has the characteristics of fast-detection, high-sensitivity and low-requirements for sample pretreatment. It plays a more and more important role in the detection of organic pollutants. In this study, MIL-101 and Au nanoparticles were prepared by hydrothermal method and aqueous solution reduction method respectively, and MIL-101/Au composite nanoparticles were prepared by electrostatic interaction. The SERS properties of the composite substrate were optimized by adjusting the size of Au nanoparticles and the surface distribution density of MIL-101 nanoparticles. The detection limit of Rhodamine 6G (R6G) for the composite substrate with the optimal ratio was investigated, which was as low as 10^{-11} M. It is proved that MIL-101/Au composite nanoparticles have high sensitivity to probe molecules. When they are applied to the detection of persistent organic pollutants, the detection limit for fluoranthene can reach 10^{-9} M and for 3,3',4,4'-tetrachlorobiphenyl (PCB-77) can reach 10^{-5} M.

Keywords: MIL-101; Au Nanoparticles; Surface-Enhanced Raman Scattering (SERS)

ARTICLE INFO

Received: 13 November 2021
Accepted: 31 December 2021
Available online: 8 January 2022

1. Introduction

Surface-enhanced Raman scattering (SERS) spectrum is a substance detection method that can provide fingerprint peak identification. It has high sensitivity and its samples are non-destructive. It has important application value in the fields of environmental chemistry, medical detection, food safety and so on[1–3]. Regarding the mechanism of SERS enhancement, there are two types to be recognized in academic: physical enhancement and chemical enhancement, in which physical enhancement is dominant. Physical enhancement is also called electromagnetic field enhancement. Under the irradiation of incident light, electrons on metal surfaces with nanostructures are excited to produce vibration, and localized surface plasmon resonance (LSPR) can be formed at a specific excitation frequency. This leads to the enhancement of the local electromagnetic field of the metal substrate and greatly enhances the Raman signal of the probe molecules attached to the metal surface.

The enhancement effect of SERS strongly depends on the metal type, nanostructure and morphology of the substrate. The traditional coin metals such as Au, Ag and Cu have been widely studied because of their excellent surface plasmon resonance characteristics[4–6]. However, some polycyclic aromatic hydrocarbons have poor affinity with the surface of traditional precious metals, resulting in weak or even no detection signal, which further limits the application of SERS in detection field. Therefore, in order to improve the affinity between probe

molecules and metal particles, the functionalization of metal nanoparticles has become a research hotspot. Introducing modifiers such as cysteamine[7] and cyclodextrin[8,9]. to modify the surface of nano metals can effectively improve the enrichment effect of molecules[10]. Now, the development trend of SERS substrate is to composite precious metals with plasma resonance effect and porous materials with adsorption and enrichment ability to build composite particles. Porous materials can effectively adsorb solution molecules. However, the application prospects of traditional activated carbon, aluminum silicate[11] and zeolite[12] are limited due to defects such as small specific surface, fixed structure and inability to be modified flexibly. As a new porous material, metal organic framework (MOF) material has the characteristics of large specific surface area, excellent adsorption capacity and adjustable structure. It has been widely studied in the field of adsorption and removal of organic molecules. In 2010, Haque *et al.*[13] first reported the study on the adsorption of dyes by MOF. For methyl orange in aqueous solution, two Cr bases MOF materials (MIL-101(Cr) and MIL-53(Cr)) showed better adsorption effect than traditional activated carbon. At the same time, the adsorption capacity of MIL-101(Cr) was more and the adsorption rate is faster. It is due to the larger specific surface area of MIL-101(Cr). In addition, the π-π interaction between MOF particles and organic molecules can enhance the adsorption of organic molecules[14], such as the adsorption of Uio-66 on herbicide methyl chlorophenoxypropionic acid (MCPP)[15]. The probe molecules can be preconcentrated near the metal surface by using the adsorption characteristics of MOF.

Generally, there are three ways to combine MOF with metal particles. One is to take metal particles as the core and MOF particles as the shell to coat its surface to construct the core-shell composite structure. Zhang *et al.*[16] obtained Au/MOF-74 core-shell structure by one-pot method to detect 4-nitrothiophene in situ. Yang *et al.*[17] synthesized Au@MIL-101 through layer by layer self-assembly to realize the detection of hexamethylene tetramine at 10^{-8} M. Au@ZIF-8 prepared by Li Shikou, *et al.*[18] showed a highly sensitive SERS response to crystal violet. The defect of this method is that the spacing of metal particles is not easy to control to get the best state of "hot spot". The second method is to prepare AuNPs/MIL-101 by in-situ reduction of metal embedded in MOF by solution impregnation method, which can achieve relatively low SERS detection limits for R6G and benzidine[19]. Because in-situ reduction cannot control the size and morphology of metal particles, it is difficult to realize SERS performance optimization. The third is to connect MOF and metal particles with modifiers, specifically to modify MOF in preparation or after MOF preparation. Then reduce the loaded metal particles at the modification position in the metal precursor solution[20], or grafted MOF particles on the modified metal surface. This synthetic method has better control over the metal loading position, but the synthesis is cumbersome. Additional reagents need to be introduced, and the cost is increased.

Therefore, this paper explores a simple and easy method which can well control the morphology and spacing of MOF and metal particles. The composite SERS substrate was prepared by combining negatively charged MIL-101 in methanol dispersion with positively charged Au particles coated with Cetyl trimethyl ammonium bromide (CTAB) by electrostatic adsorption. Mil-101 provides adsorption and enrichment of probe molecules, while Au particles provide surface electromagnetic enhancement. The substrate enhancement ability is optimized by adjusting the size of Au particles and the load density on the surface of MIL-101. When the particle size of Au particles is 60 nm and the composite volume ratio of MIL-101 to Au is 1:2, the SERS substrate gets the best performance. In the end, SERS substrate with best performance is applied to the detection of fluoranthene and PCB-77. It is found that the detection limit of the substrate for typical persistent organic pollutant fluoranthene can reach 10^{-9} M and 10^{-5} M for PCB-77, which has important research significance and application value in the field of real-time and highly sensitive detection of environmental persistent organic

pollutants.

2. Experiment parts

2.1 Preparation of MIL-101/Au composite nanoparticles

2.1.1 Laboratory reagent

The main reagents used in the experiment are shown in **Table 1**.

Table 1. Main reagents used in the experiment

Name	Factories	Purity
Chromium (III) nitrate nonahydrate	Aladdin	AR
Terephthalic acid	China National Pharmaceutical Group Corporation	99%
Hydrofluoric acid	Tianjin Tianli Chemical Reagent Co., Ltd	40%
Gold acid chloride trihydrate	Aladdin	AR
Sodium borohydride	Shanghai Sinopharm reagent	98.0%
Cetyl trimethyl ammonium bromide (CTAB)	Tianjin Kaitong Chemical Reagent Co., Ltd	99%
Anhydrous ethanol	Tianjin Damao Chemical Reagent Co., Ltd	99.7%
N,N-dimethyl formamide	Aladdin	99.8%
Methanol	Tianjin Damao Chemical Reagent Co., Ltd	AR

2.1.2 Preparation of MIL-101

Chromium (III) nitrate nonahydrate (5 mmol), terephthalic acid (5.2 mmol) and pure water (30 mL) were added to a 50 mL beaker for ultrasound for 30 min, and then 0.25 mL hydrofluoric acid was added. The mixed solution was transferred to a reactor with tetrafluoroethylene lining and maintained at 220 ℃ for 8 h. After the reaction, cool down naturally to room temperature. Wash the product alternately with ethanol and N,N-dimethyl formamide (DMF) for three times to remove the incompletely reacted terephthalic acid. Reflux with ethanol solution at 85 ℃ for 6 h to remove the residual reactants in the MOF channel. Finally, wash it twice with anhydrous ethanol and keep it in a vacuum oven at 150 ℃ for 12 h. Green powder was obtained after drying, and then dispersed in methanol solution to prepare 0.1 mg/mL suspension.

2.1.3 Preparation of Au nanoparticles

Au nanoparticles were prepared by seed growth method. Au seed preparation: first, prepare a certain amount of 0.01 M $HAuCl_4$ and 0.1 M CTAB aqueous solution, mix 0.25 mL $HAuCl_4$ and 7.5 mL CTAB solution evenly, and quickly add cold newly prepared $NaBH_4$ (0.6 mL, 0.01 M) aqueous solution, stirring at high speed for 1 min to obtain gold seed suspension, and then set aside at room temperature for 1 h. Preparation of growth solution: mix CTAB (6.4 mL, 0.1 M) and $HAuCl_4$ (0.8 mL, 0.01 M) solution. Add AA (3.8 mL, 0.1 M) and 32 mL ultrapure water. Finally, add 10, 20, 30 and 40 μL gold seeds diluted 10 times into the growth solution respectively. Gold particle solutions with different particle sizes are obtained after setting aside for 4 h. Wash them twice with ultrapure water, and then disperse them in 8 mL methanol solution for standby.

2.1.4 Preparation of MIL-101/Au composite nanoparticles

The suspension of MIL-101 and Au was mixed at different volume ratios (1:1, 1:2 and 1:3) under high-speed stirring for 5 min and stood for 1 h to obtain composite particles with different Au loading densities.

2.2 Characterization and test method of MIL-101/Au composite substrate

The particle morphology and crystal structure are determined by the scanning electron microscope (SU-8010, 10 kV) of Hitachi, Japan, and German Bruker X-ray diffractor (D8ADVANCE, emission source of Cu Kα line, acceleration voltage of 35 kV, and scanning angle of 5–70°) and Nicolet IS50 Fourier Transform Infrared Spectroscopy (FTIR, scan wavenumber ranging from 500–3,500 cm^{-1}) of Thermo Fisher, Inc. Ultraviolet visible absorption spectrum (UV-vis) is measured by ultraviolet spectrophotometer (model: Carry500) of Agilent company.

During the SERS performance test, take 0.2 mL R6G and PCB-77 solutions with different concentrations and 0.8 mL suspension of compo-

site particles. After the composite particles fully adsorb the substance to be tested, remove the free molecules, and suck 20 μL with a pipette gun and drop on the silicon wafer. After vacuum drying, Raman measurement was carried out in Renishaw Invia laser micro confocal Raman spectrometer of Renishaw company in the UK. The laser wavelength was 785 nm, the acquisition time was 10 s and the laser power was 1.5 mW.

3. Results and discussion

3.1 Preparation and characterization of MIL-101/Au

Figure 1(a, b) shows the SEM morphology of MIL-101/Au composite nanoparticles under different test multiples. It can be seen from the figure that Au nanoparticles are evenly distributed on the surface of MIL-101, which proves the successful recombination of the two particles from the perspective of morphology.

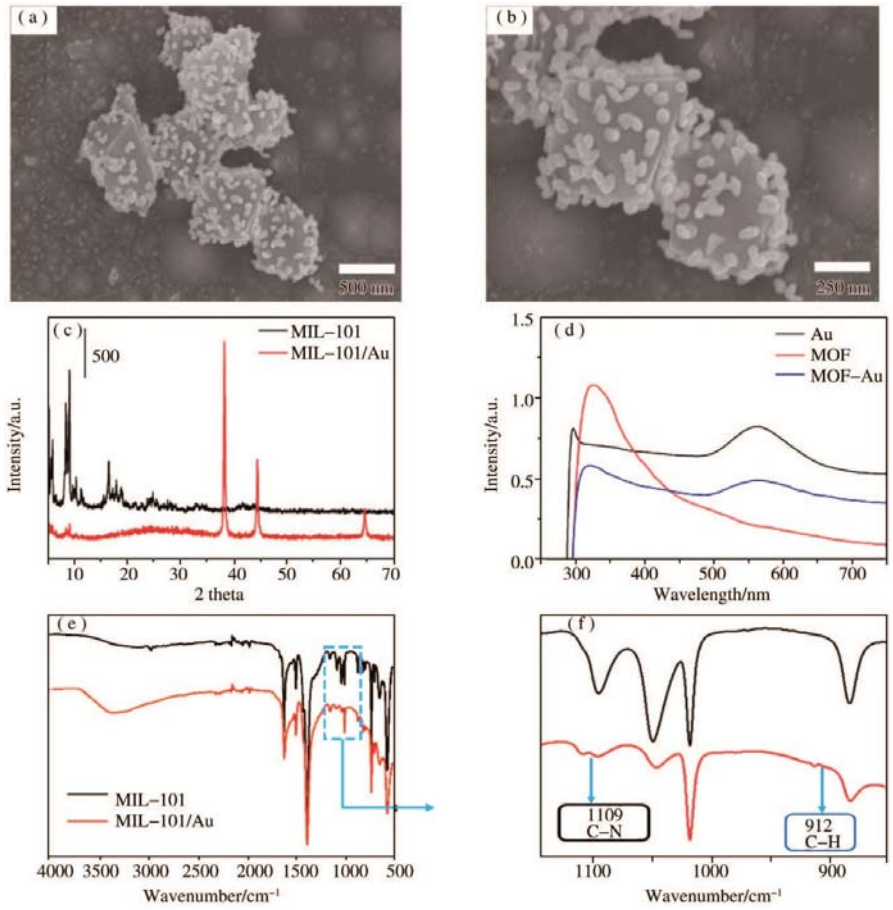

Figure 1. (a, b) SEM images of MIL-101/Au composite nanoparticles at different magnification; **(c)** XRD test diagram; **(d)** UV visible spectrum curve; **(e, f)** FTIR curve.

It can be seen from **Figure 1(c)**, the X-ray diffraction peaks of MIL-101 are mainly concentrated in the range of 5–20°. After compounding with Au nanoparticles, obvious characteristic diffraction peaks belonging to Au particles appear, in which the (111), (200) and (220) crystal planes of Au correspond to 38.2°, 44.4° and 64.6° respectively. Meanwhile, the characteristic peaks attributed to MIL-101 after recombination of particles are particularly weak, which is due to the weakening of the signal of MIL-101 against the strong characteristic peaks of Au. However, these two characterization methods cannot fully express the binding effect of MIL-101 and Au. Therefore, with the help of UV-vis spectrum, the spectral absorption peaks of MIL-101, Au and the suspension after recombination are studied. **Figure 1(d)** shows the UV spectral curves of MIL-101 and Au particles alone and after recombination. It can be seen from the figure that the absorption peak of Au particles with particle size of 60 nm is at 590 nm and the absorption peak of

MIL-101 is at 319 nm. After the two are combined, the characteristic absorption peaks of the composite particles appear near the positions of the two absorption peaks at the same time, which only produces a small blue-shift, indicating that the combination of the two by electrostatic adsorption has no effect on their respective characteristics. Therefore, the successful recombination of MIL-101 and Au is proved from the perspective of microstructure. In order to further investigate the interaction between MIL-101 and Au nanoparticles, the infrared spectrum of the composite particles and pure MIL-101 is analyzed. **Figure 1(f)** is the enlarged local spectrum of **Figure 1(e)**. According to the comparison of the infrared spectrum curves before and after composite, the composite particles appear new absorption peaks at 1,109 and 912 cm^{-1}, which belongs to the vibrational absorption of C-N bond and C-H bond respectively. They all come from CTAB molecules coated on the surface of Au particles. This shows that there is no new chemical bond formed in the recombination process of MIL-101 and Au, and the binding process is a physical change.

3.2 Optimization of SERS performance

The SERS effect strongly depends on the morphology, size and particle gap of metal nanostructures. In this experiment, the surface plasmon resonance effect of composite particles was adjusted by controlling the size and distribution density of Au nanoparticles on the surface of MIL-101, so as to optimize the SERS performance of particles.

The particle size of Au particles is adjusted by changing the amount of seed dispersion added to the growth solution. **Figure 2(a)** shows the UV-vis spectra of Au particle dispersion with different particle sizes. It can be seen from the figure that with the increase of Au particle size from 40 nm to 60 nm, the absorption peak shifts red and the peak width is relatively narrow, which shows that the particle size distribution is uniform. When the particle size increases to 70 nm, the absorption peak becomes wider and the particle size distribution begins to be uneven. The Au particles with four particle sizes are compounded with MIL-101 dispersion in a volume ratio of 1:1, and the compounded particles are used as the substrate for SERS performance test. **Figure 2(b)** shows the results of SERS detection for R6G at 10^{-5} M. **Figure 2(c)** shows the Raman signal intensity of each substrate in **2(b)** at 1,509 cm^{-1}. It can be seen from the figure that the signal intensity of gold particles with particle size of 60 nm is the largest and the SERS performance is the best. Therefore, it is used as the optimal substrate for subsequent experimental research.

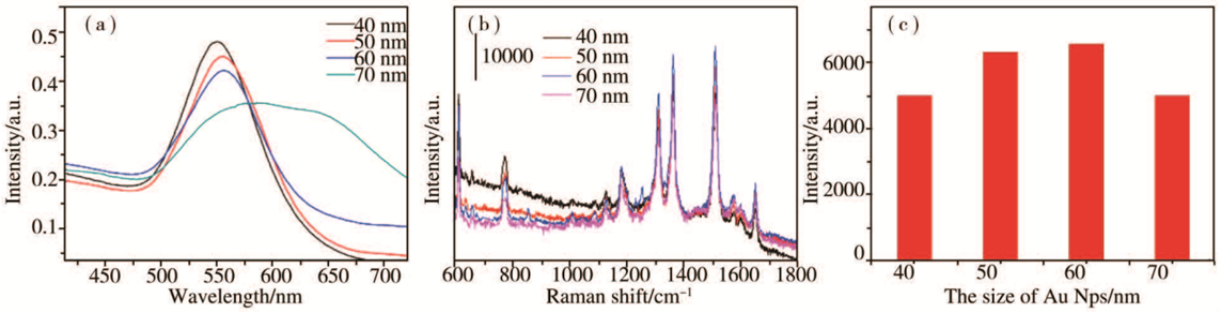

Figure 2. (a) UV-vis spectra of Au particle dispersion with different particle sizes; **(b)** SERS test of R6G by composite particles corresponding to Au nanoparticles with different particle sizes; **(c)** corresponding to the Raman signal intensity at 1,509 cm^{-1} in **(b)**.

When determining the size of Au nanoparticles, another factor, that is, the distribution density of Au particles on MIL-101, was investigated. The distribution density of Au particles was adjusted by controlling the volume ratio of MIL-101 to Au nanoparticle dispersion. Taking 60 nm Au particles as the precursor, three substrates were prepared with the volume ratio of MIL-101 to Au particles of 1:1, 1:2 and 1:3 respectively. The SERS properties were investi-

gated with 10^{-5} M R6G as the probe molecule. **Figure 3(a, b** and **c)** is the SEM diagram of the particles compounded according to the three volume ratios. It can be seen from the figure that with the increase of Au addition from 1:1 to 1:2, the Au particle density increases significantly after composite. Continuing to increase to 1:3, Au particle density no longer increases significantly after composite. **Figure 3(d)** shows the SERS performance diagram of R6G test of three substrates. **Figure 3(e)** shows the Raman signal intensity at 1,509 cm^{-1} in **3(d)**. It can be seen from the SERS performance diagram that the Raman signal is significantly enhanced with the addition of Au particles from 1:1 to 1:2, which is due to the increase of Au particle density. On one hand, the increase of Au particle density can increase more surface "hot spots"; on the other hand, reducing the spacing between particles will produce stronger surface plasma coupling and stronger surface electromagnetic field effect. With the further increase of the amount of Au particles, the loading density of Au particles is saturated and the Raman signal intensity is basically stable. This is because there is an electrostatic balance between MIL-101 and Au particles, i.e. potential "zero". This is also a major advantage of electrostatic interaction to avoid the formation of particle accumulation due to excessive Au particle density, which will affect the Raman enhancement effect. Therefore, the volume ratio 1:2 of MIL-101 to Au particles is regarded as the optimal composite ratio for the next performance study.

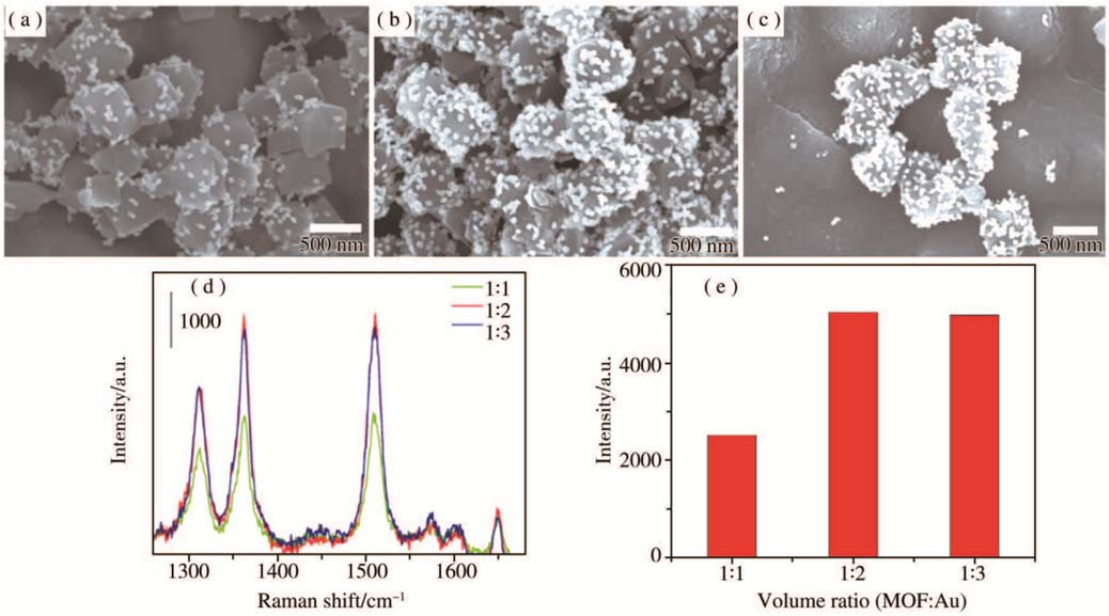

Figure 3. SEM diagram of MIL-101 and Au compounded according to volume ratio: **(a)** 1:1; **(b)** 1:2; **(c)** 1:3. **(d)** SERS test of R6G after compounding according to different volume ratio; **(e)** corresponding to the Raman signal intensity at 1,509 cm^{-1} in **(d)**.

3.3 Study on SERS performance

In order to explore the Raman enhancement mechanism of the substrate, Raman tests were carried out on 10^{-5} M R6G molecules on three types of substrates: pure silicon wafer, MIL-101 and MIL-101/Au composite particles. The results are shown in **Figure 4(a)**. Almost no R6G Raman signal appeared on the pure silicon wafer. After the introduction of MOF, due to its porous and adsorption characteristics, R6G molecules are enriched, the number of R6G molecules per unit volume is significantly increased, and weak signal peaks will appear. Further, after MOF and Au are combined, the R6G signal is significantly enhanced by combining the characteristics of MOF materials and the surface plasma coupling effect of precious metal gold particles. Due to the introduction of MOF materials, the adsorption of probe molecules takes a certain time. Therefore, the effect of adsorption time on the SERS performance of MIL-101/Au composite substrate is further explored. **Figure 4(b)** shows the Raman

spectrum curve of MIL-101/Au substrate on R6G under different adsorption time. **Figure 4(c)** shows the change curve of peak intensity over time at 1,509 cm^{-1} in corresponding **4(b)**. Obviously, when the adsorption time is extended, the Raman detection signal of the corresponding substrate will increase, but after the adsorption time reaches 40 min or even longer, the corresponding signal intensity will hardly change, indicating that when the adsorption time is 40 min, and the substrate reaches adsorption saturation on the probe molecules, the number of probe molecules that can effectively interact with the substrate will not increase, and the Raman signal of the corresponding molecules will not be enhanced. After various substrate indexes have been determined, Raman tests are carried out on R6G molecules of different concentrations on the composite substrate. As shown in **Figure 4(d)**, the detection limit of R6G by the substrate can reach 10^{-11} M. It has reached the leading level in the reported literature.

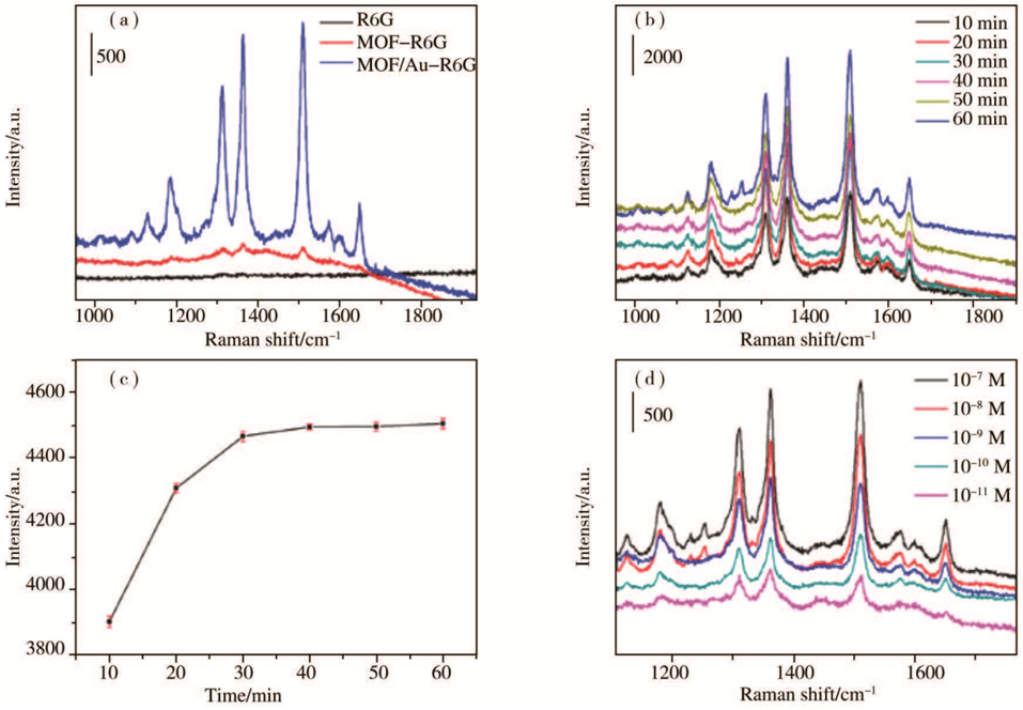

Figure 4. **(a)** Raman spectra of R6G on different substrates; **(b)** Raman spectra of R6G by MIL-101/Au at different adsorption times; **(c)** corresponding to the relationship between Raman signal intensity and adsorption time at 1,509 cm^{-1} in **(b)**; **(d)** Raman detection spectrum curve of MIL-101/Au composite substrate for different concentrations of R6G.

3.4 Study on detection and application of sustainable organic pollutants

A large number of persistent organic environmental pollutants such as polychlorinated biphenyls (PCBs) have the characteristics of strong toxicity and easy bioaccumulation, which seriously threaten human health and the environment. Therefore, the research on rapid trace detection and efficient treatment of persistent organic pollutants is very urgent. In order to further explore the practical application of composite substrate, in this experiment, Raman detection was carried out for two typical organic pollutants: fluoranthene and PCB-77. The test results are shown in **Figure 5(a)** and **Figure 5(c)**. The detection limit of the prepared composite substrate for fluoranthene can reach 10^{-9} M and PCB-77 can reach 10^{-5} M, successfully realizing the trace detection of POPs. **Figures 5(b)** and **(d)** show the plots of the concentration logarithm and Ramanan peak intensity of fluoranthene and PCB-77, respectively. It can be seen from the figure that the Raman peak intensity of PCB-77 at 1,599 cm^{-1} shows a good linear correlation with its logarithm of concentration, and the correlation index R^2 can reach 0.993. For fluoranthene, the correlation between the characteristic Raman peak intensity and the concentration logarithm is relatively poor, indicating that although the detection limit of the substrate for fluoranthene is lower,

the detection stability of the substrate is worse than that of the substrate for PCB-77, which means that there are still difficulties to be overcome in the detection and application of persistent organic compounds.

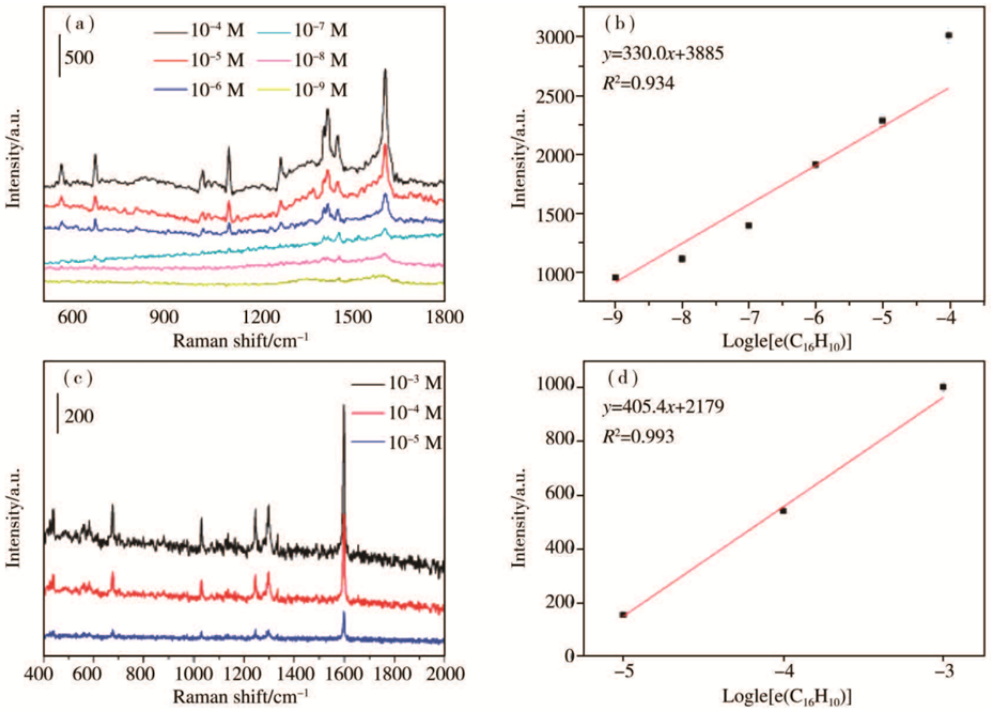

Figure 5. **(a)** Raman detection curves of different concentrations of fluoranthene on MIL-101/Au composite substrate; **(b)** the relationship between fluoranthene concentration and Raman peak intensity (1,607 cm^{-1}); **(c)** Raman detection curves of substrate to different concentrations of PCB-77; **(d)** relationship between PCB-77 concentration and Raman peak intensity (1,599 cm^{-1}).

4. Conclusion

In this paper, the combination of MIL-101 and Au nanoparticles was successfully realized by electrostatic adsorption. Combining the advantages of the two materials, the high sensitive detection of persistent organic pollutants such as fluoranthene and polychlorinated biphenyls is realized by using the excellent molecular enrichment ability of MIL-101 and the significant plasma resonance coupling effect of Au nanoparticles. The detection limit of fluoranthene can reach 10^{-9} M and PCB-77 can reach 10^{-5} M. Through the physical adsorption of MIL-101 and π-π conjugation with organic pollutants, it promotes the interaction between substrate and detector, and makes up for the poor adsorption capacity, weak or no detection signal of traditional noble metal SERS substrate for polycyclic aromatic hydrocarbons. This paper proves that MIL-101/Au composite SERS substrate has important research significance and application value in the fields of food safety, environmental monitoring, etc.

Conflict of interest

The authors declare that they have no conflict of interest.

Acknowledgements

Youth Project of National Natural Science Foundation of China (51701186); supported by the key R & D program of Shanxi Province (201603D421030).

References

1. Wong CL, Dinish US, Schmidt MC, *et al*. Non-labeling multiplex surface enhanced Raman scattering (SERS) detection of volatile organic compounds (VOCs). Analytica Chimica Acta 2014; 844: 54–60.
2. Indrasekara ASDS, Meyers S, Shubeita S, *et al*. Gold nanostar substrates for SERS-based chemical sensing in the femtomolar regime. Nanoscale 2014; 6(15): 8891–8899.
3. Wang Y, Lee K, Irudayaraj J. Silver Nanosphere SERS Probes for sensitive identification of pathogens. The Journal of Physical Chemistry C

2010; 114(39): 16122–16128.
4. Bian J, Shu S, Li J, *et al*. Reproducible and recyclable SERS substrates: Flower-like Ag structures with concave surfaces formed by electrodeposition. Applied Surface Science 2015; 333: 126–133.
5. Bell SJ, McCourt M. SERS enhancement by aggregated Au colloids: Effect of particle size. Physical Chemistry Chemical Physics 2009; 11(34): 7455–7462.
6. Zhao B, Lu Y, Zhang Y, *et al*. Silver dendrites decorated filter membrane as highly sensitive and reproducible three dimensional surface enhanced Raman scattering substrates. Applied Surface Science 2016; 387: 431–436.
7. Kang L, Xu P, Chen D, *et al.* Amino acid-assisted synthesis of hierarchical silver microspheres for single particle surface-enhanced Raman spectroscopy. The Journal of Physical Chemistry C 2013; 117(19): 10007–10012.
8. Strickland AD, Batt CA. Detection of carbendazim by surface-enhanced Raman scattering using cyclodextrin inclusion complexes on gold nanorods. Analytical Chemistry 2009; 81(8): 2895–2903.
9. Li F, Wang J, Lai Y, *et al.* Ultrasensitive and selective detection of copper (II) and mercury (II) ions by dye-coded silver nanoparticle-based SERS probes. Biosensors & Bioelectronics 2013; 39(1): 82–87.
10. Liu J, White I, DeVoe DL. Nanoparticle-functionalized porous polymer monolith detection elements for surface-enhanced Raman scattering. Analytical Chemistry 2011; 83(6): 2119–2124.
11. Liu R. Study on the removal of phenol in coking wastewater by coagulation with composite flocculants [Master's thesis]. Taiyuan: North University of China; 2018.
12. Su Y. A study on the adsorption of anionic dye and micro-molecular organics by cationic agents modified zeolite [Master's thesis]. Zhengzhou: Zhengzhou University; 2014.
13. Haque E, Lee JE, Jang IT, *et al*. Adsorptive removal of methyl orange from aqueous solution with metal-organic frameworks, porous chromium-benzenedicarboxylates. Journal of Hazardous Materials 2010; 181(1-3): 535–542.
14. Khan NA, Jhung SH. Adsorptive removal and separation of chemicals with metal-organic frameworks: Contribution of π-complexation. Journal of Hazardous Materials 2017; 325: 198–213.
15. Seo YS, Khan NA, Jhung SH. Adsorptive removal of methylchlorophenoxypropionic acid from water with a metal-organic framework. Chemical Engineering Journal 2015; 270: 22–27.
16. Zhang Y, Hu Y, Li G, *et al*. A composite prepared from gold nanoparticles and a metal organic framework (type MOF-74) for determination of 4-nitrothiophenol by surface-enhanced Raman spectroscopy. Microchimica Acta 2019; 186(7): 477.
17. Cai Y, Wu Y, Xuan T, *et al.* Core-shell Au@metal-organic frameworks for promoting raman detection sensitivity of methenamine. ACS Applied Materials & Interfaces 2018; 10(18): 15412–15417.
18. Li Q, Gong S, Huang F, *et al.* Tailored necklace-like Ag@ZIF-8 core/shell heterostructure nanowires for high-performance plasmonic SERS detection. Chemical Engineering Journal 2019; 371: 26–33.
19. Hu Y, Liao J, Wang D, *et al.* Fabrication of gold nanoparticle-embedded metal-organic framework for highly sensitive surface-enhanced Raman scattering detection. Analytical chemistry 2014; 86(8): 3955–3963.
20. Xuan T, Gao Y, Cai Y, *et al*. Fabrication and characterization of the stable Ag-Au-metal-organic-frameworks: An application for sensitive detection of thiabendazole. Sensors and Actuators B: Chemical 2019; 293: 289–295.